ChemistryOpen

Full Papers
doi.org/10.1002/open.202000336

**Chemistry
Europe**
European Chemical
Societies Publishing

Aggregation Behavior of Poly(Acrylic acid-co-Octadecyl Methacrylate) and Bovine Serum Albumin in Aqueous Solutions

Mengmeng Zhou,[a, b] Yutong Bi,[c] Haijun Zhou,[b] Xiaoqi Chen,[b] Fen Zhang,[b] Yantao Li,*[b] and Xiongwei Qu*[a]

Polymer-protein complexing systems have been extensively studied because of their wide application in biomedicine and industry. Here, we studied the aggregation behavior of the hydrophobically associating water-soluble polymer poly(acrylic acid-co-octadecyl methacrylate) [P(AA-co-OMA)] prepared with nonionic surfactant as an emulsifier and bovine serum albumin (BSA) in aqueous solution. We identified the optimal composite conditions of P(AA-co-OMA) and BSA aqueous solution. We measured the zeta potential, dynamic light-scattering particle size, and surface tension of P(AA-co-OMA) and BSA mixed aqueous solution. The results showed that the aggregation behavior between the polymer and BSA relied mainly on the hydrophobic interactions between the molecules. In addition, the best compounding condition was 8 wt.% of P(AA-co-OMA) content. The structure of hydrophobically associating polymer P(AA-co-OMA) and its aggregation with BSA were characterized by Fourier-transform infrared spectroscopy. The infrared spectroscopy results identified the hydrogen bonding behavior of the amino and carboxyl groups between the polymer and BSA. This behavior was also confirmed using thermogravimetric analysis and differential scanning calorimetry. The thermal decomposition temperature and melting temperature of BSA changed before and after it was combined with the polymer. We measured the morphology of the polymer BSA aggregate with 8% polymer content by transmission electron microscopy. The binding mechanism was investigated, as well.

1. Introduction

The binding of polymers to proteins has been extensively studied in the last decades.[1] The self-assembled particles of water-soluble protein biomacromolecules and polyanion polymers have attracted the attention of many researchers in the field of biomaterials and nanoscience, including applications with functional polymers.[2] These polymers have been widely used in new membrane materials, protein separation, molecular self-assembly, controlled drug release,[3] and the fields of nanocatalysis[4] and immunology.[5] Covalent bond coordination is an effective way for polyanion polymers and proteins to form complexes.[6] Many polymers and functional biomacromolecules do not have functional bonds. They usually need to be modified, and the modified carrier biomacromolecules often have adverse effects on living systems.[7] Therefore, noncovalent bond interactions between polymers and proteins, including hydrogen bond binding, van der Waals force, hydrophobic interactions, and ionic interactions, have attracted the attention of researchers.[8] The combination of polymer and protein is expected to be used in biology. Therefore, the selection of polymer is particularly important. Polyacrylic acids are polymers with excellent biocompatibility and have been widely used in the field of medicine, including carbomer,[9] eudragit, and polyvinyl pyrrolidone biopolymer for dry eye treatment.[10] The application of polyacrylate polymer in subunit vaccines also is being studied.[11] Polymethylmethacrylate has attracted attention in the field of biomedical materials and vaccine adjuvants because of its excellent biocompatibility and nontoxic characteristics.[12] Hilgers found that polyacrylic acid alkyl ester has a strong secondary immune response, which is expected to replace oil adjuvant and avoid the side effects of mineral oil.[13] Therefore, the application of polyacrylic acid polymer materials in biomedicine and immunology is worthy of further exploration. Mustafaev has studied noncovalent bonds between PAA and bovine serum albumin (BSA). The results showed that the electrostatic force between PAA and BSA is the main driving force to realize self-assembly.[14] Researchers have introduced metal ions to confirm that the ion coordination complex of PAA and protein has obvious immunogenicity and immunoprotection and is an artificial polymer antigen vaccine.[15] A few years ago, polyacrylic acid was grafted with long alkyl chains and its aggregation properties were studied. The polymer in this

[a] M. Zhou, Prof. X. Qu
     School of Materials Science and Engineering
     Hebei University of Technology
     300130, Tianjin (China)
     E-mail: xwqu@hebut.edu.cn
[b] M. Zhou, Prof. H. Zhou, X. Chen, Prof. F. Zhang, Prof. Y. Li
     Institute of Energy Resources
     Hebei Academy of Sciences
     050081, Shijiazhuang, Hebei Province (China)
     E-mail: 13903116163@163.com
[c] Y. Bi
     School of Materials Science and Engineering
     Hebei University of Science and Technology
     050000, Shijiazhuang, Hebei Province (China)

ChemistryOpen

Full Papers
doi.org/10.1002/open.202000336

Chemistry Europe
European Chemical
Societies Publishing

system is a hydrophilic long link branch hydrophobic alkyl chain; its rheological properties were studied.[16]

Hydrophobically associating water-soluble polymer (P(AA-co-OMA)) refers to a water-soluble polymer derivative[17] that remains soluble in water by introducing a few hydrophobic groups into the water-soluble polymer. P(AA-co-OMA) has characteristics of micro-phase separation, which makes it form polymer micelles, polymer vesicles, polymer multimolecular aggregates, and physical crosslinking networks in aqueous solution. There are significantly different structures and properties from conventional water-soluble polymers.[18] Because of their long hydrophobic chain, P(AA-co-OMA)s can also have hydrophobic effects when there are hydrogen bonds or electrostatic interactions with BSA. Therefore, in this study, we selected acrylic acid as a hydrophilic monomer because of its potential application in vaccine. Octadecyl methacrylate was selected as a hydrophobic chain segment to prepare a hydrophobically associating polymer poly(acrylic acid-co-octadecyl methacrylate) – a micro-block copolymer. Research on this P(AA-co-OMA) and BSA aggregation has had great significance for the future use of this polymer in immunology.

This new system, including P(AA-co-OMA)-BSA, is based on the following considerations: (1) the main interest is to obtain polymer protein aggregates suitable for biological applications; (2) natural proteins have been used as drug carriers in recent years; and (3) the combination of the hydrophobic association materials and proteins will provide theoretical support for later applications in immunology. Generally, drug delivery materials rely on polymer nanoparticles (the preparation method is as follows: spray drying method, solvent emulsification/evaporation, ionic crosslinking, and polymerization) for drug delivery,[19] which has attracted significant attention. The methods, however, are limited in their application and production, including a complex production process and the high cost of the final product.[20] In this study, the combination of hydrophobically associating polymer and protein relied on the hydrophobic association and hydrogen bonding force, which offered the advantages of a simple production process and easy industrialization in future production. This system is expected to be used in the field of vaccination and as an antigen delivery system for immunity.

We report a poly(acrylic acid-co-octadecyl methacrylate) hydrophobically associating aqueous solution prepared through nonionic surfactant as the emulsifier; the aggregation behavior with BSA was studied. We characterized its aqueous solution performance by PSS-Z3000 and a contact angle-measuring instrument. We also confirmed the hydrogen bonding between a hydrophobic association polymer and protein by Fourier-transform infrared spectroscopy (FTIR), thermogravimetric analysis (TGA), and differential scanning calorimetry (DSC). We characterized the aggregation morphology of P(AA-co-OMA)-BSA using transmission electron microscopy (TEM).

2. Results and Discussion

2.1. FTIR Spectroscopic Analysis of Hydrophobically Associating Poly(Acrylic Acid-co-octadecyl Methacrylate)

In this study, we selected acrylic acid as a hydrophilic monomer, octadecyl methacrylate as a hydrophobic monomer, and non-ionic surfactant as an emulsifier to prepare the hydrophobic association polymer. The infrared spectrum analysis of the polymer is shown in Figure 1.

Figure 1 shows the infrared spectrum of hydrophobically associating polymer poly(acrylic acid-co-octadecyl methacrylate) [P(AA-co-OMA)]. A very wide characteristic absorption peak is evident at 3060–3679 cm^{-1}, which is the absorption peak of the remaining incompletely neutralized carboxyhydroxyl group in the polymer. Peaks at 2943 cm^{-1} and 2856 cm^{-1} correspond to the asymmetric and symmetric stretching vibration absorption peaks of methylene. Peaks at 1791 cm^{-1} and 1157 cm^{-1} are symmetric and asymmetric stretching characteristic peaks of ester group. The peak at 1684 cm^{-1} is a characteristic absorption peak of the carbonyl group. The peak at 1470 cm^{-1} is the methyl and methylene and bending vibration characteristic peaks, 763 cm^{-1} is the methylene in-plane shaking vibration characteristic peak, and 1546 cm^{-1} was the characteristic absorption peaks of carboxylate (–COO–). These peaks are seen in the figure and not only are characteristic absorption peaks of octadecyl methacrylate but also characteristic peaks of sodium acrylate obtained by neutralization of acrylic acid by sodium hydroxide. We did not observe an obvious absorption peak of the C=C double bond at 1630 cm^{-1}. This proved that the structure of the polymer, which was mixed with BSA to study the binding mechanism.

2.2. Effect of P(AA-co-OMA) Content on Zeta Potential of P(AA-co-OMA)-BSA Systems

Zeta potential can characterize the stability of colloidal dispersion systems. In this study, we selected the 1 wt.% P(AA-
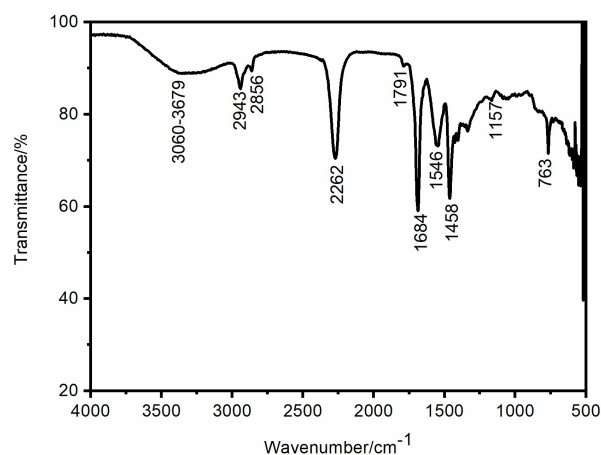

Figure 1. FTIR spectra of hydrophobically associating polymer poly(acrylic acid-co-octadecyl methacrylate).

ChemistryOpen

Full Papers
doi.org/10.1002/open.202000336

Chemistry
Europe
European Chemical
Societies Publishing

co-OMA)/BSA solutions to test the zeta potential at different pH values to change the mass ratio of P(AA-co-OMA) to BSA, and the percentages of P(AA-co-OMA) in the P(AA-co-OMA)/BSA system were 0 wt.%, 2 wt.%, 4 wt.%, 6 wt.%, 8 wt.%, 10 wt.%, 12 wt.%, and 14 wt.%. The results are shown in Figure 2.
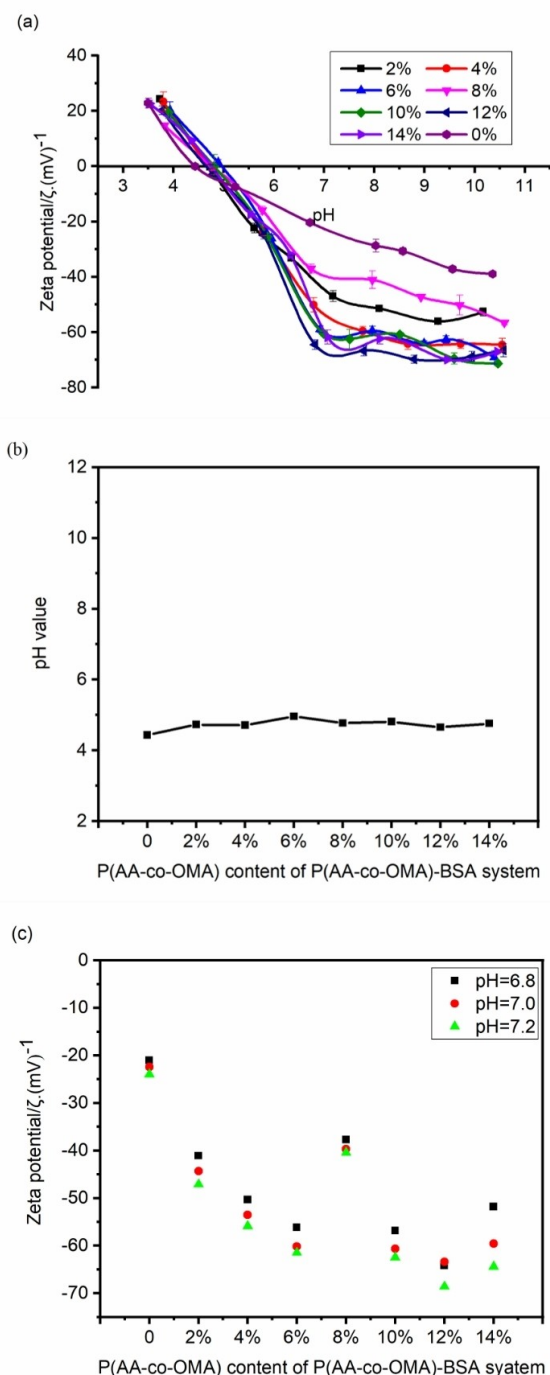

Figure 2. The evaluation of the zeta potential of different P(AA-co-OMA) content of P(AA-co-OMA)-BSA system: (a) zeta potential of P(AA-co-OMA)-BSA system taking pH and composition as a function; (b) isoelectric point (pH value when zeta potential is equal to zero) of different P(AA-co-OMA) content of P(AA-co-OMA)-BSA system; and (c) zeta potential of different compositions at three pH values (pH = 6.8, 7.0, 7.2).

The evaluation of zeta potential of P(AA-co-OMA)-BSA system as a function of pH and composition is shown in Figure 2(a). It is intuitive to show the change trend of zeta potential with P(AA-co-OMA) content and pH value. The isoelectric point of the P(AA-co-OMA)-BSA aqueous solutions is shown in Figure 2(b). The isoelectric point of 1 wt.% BSA aqueous solution is 4.4, and the isoelectric points of 1 wt.% P(AA-co-OMA)/BSA aqueous solutions were all higher than 4.4 and less than 5.0.

This study provides the basis for future vaccine adjuvant development. The pH value of vaccine adjuvant is generally between 6.8 and 7.2. Therefore, we selected three pH values for analysis of the zeta potential, as shown in Figure 2(c). The zeta potential absolute value was a minimum of 8% proportion of P(AA-co-OMA) between 2 wt.% and 14 wt.%. When the polymer content was between 2 wt.% and 8 wt.%, the polymer and BSA showed a relatively loose aggregation state. The zeta potential absolute value was increased because of the increase in the polymer surface charge. When the polymer content reached 8%, strong and stable aggregates were formed, and the surface charges in the aggregates were reduced, which was the result of the strong hydrophobic binding and hydrogen bonding between the polymer and BSA. With increasing polymer content, the excess surface charges on the polymer were exposed. The zeta potential absolute value was then increased. Therefore, in the following tests, we selected pH 6.8. The analysis and tests were all above the isoelectric point of the mixtures; the system then remained stable, and it was not easy to separate polymers.

2.3. Effect of P(AA-co-OMA) Content on Dynamic Light-Scattering Particle Size of P(AA-co-OMA)-BSA Aqueous Solutions

Dynamic light-scattering particle size parameters can be used to represent the average particle size and particle size distribution of the P(AA-co-OMA)/BSA aggregate system. Here, we prepared a 0.25 wt.% P(AA-co-OMA) aqueous solution and 2.5 wt.% BSA aqueous solution into a 1 wt.% P(AA-co-OMA)-BSA aqueous solution with weight fraction ratios of P(AA-co-OMA) in P(AA-co-OMA)/BSA of 2 wt.%, 4 wt.%, 6 wt.%, 8 wt.%, 10 wt.%, 12 wt.%, and 14 wt.%. The particle sizes by dynamic light scattering are shown in Figure 3.

With increasing P(AA-co-OMA) content, the particle size first became smaller and then increased. When the polymer content was 8 wt.%, the average particle size was the smallest and the distribution was narrow. The BSA and P(AA-co-OMA) would partially bind after physical mixing at 2 wt.%, 4 wt.%, and 6 wt.% proportion. This phenomenon occurs because a higher polymer content led to more alkyl hydrophobic chains – this enhanced the ability of the alkyl hydrophobic chains to combine with the hydrophobic group of BSA to form aggregates. The best aggregation proportion was 8% polymer content. The hydrophobic region of the polymer and the hydrophobic region of the BSA were completely gathered together, and the particle size of the system was the smallest.
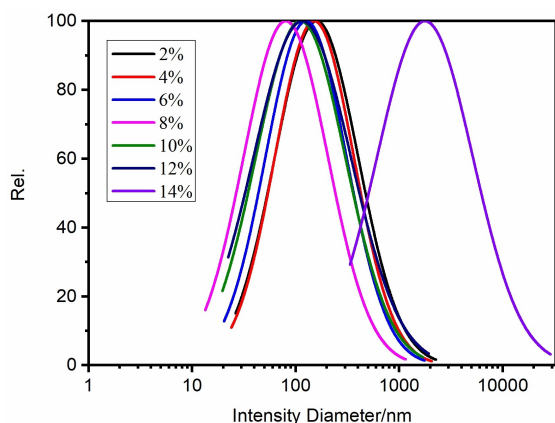
ChemistryOpen

Full Papers
doi.org/10.1002/open.202000336

Chemistry Europe
European Chemical
Societies Publishing

Figure 3. Dynamic light scattering for particle size in P(AA-co-OMA)-BSA aqueous solutions with different P(AA-co-OMA) content. A series of 1 wt.% P(AA-co-OMA)/BSA mixtures with the weight fraction ratio of pure P(AA-co-OMA) in the P(AA-co-OMA)/BSA system was 2 wt.%, 4 wt.%, 6 wt.%, 8 wt.%, 10 wt.%, 12 wt.%, and 14 wt.%.

Hydrophobic segments aggregated because of the intermolecular hydrophobic association interactions and hydrogen bonding interactions, resulting in increasing system viscosity. When the polymer content reached 14%, the extra hydrophobic segments began to crosslink and aggregate, which made the volume larger. That reaction explained the sudden change when the polymer content was 14%.

2.4. Effect of P(AA-co-OMA) Content on the Surface Tension of P(AA-co-OMA)-BSA Aqueous Solutions

According to the particle size and zeta potential results, the best aggregation result was obtained at 8 wt.%, because the polymer contained hydrophobic chains. More hydrophobic groups led to a greater decrease in surface tension. The surface tension of the system was measured at pH 6.8 (Figure 4)
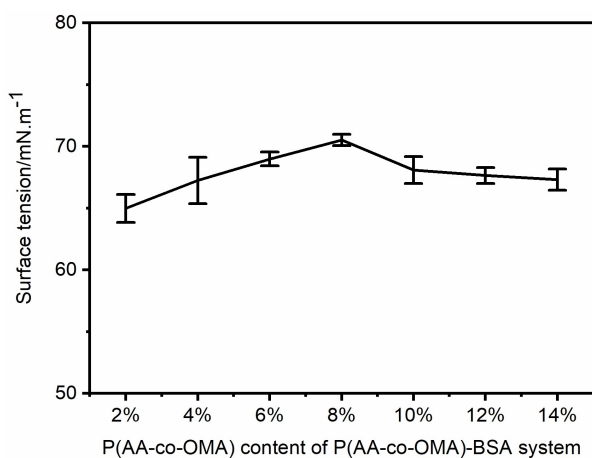
The hydrophobic alkyl chain in the system increased with increasing P(AA-co-OMA) content, and the surface tension increased with P(AA-co-OMA) concentration from 2 wt.% to 8 wt.% and decreased from 8 wt.% to 14 wt.%. There is a gradual decreasing trend to increased performance. Polymer and BSA were equivalent to anionic surfactants and amphoteric surfactants, respectively, in aqueous solution. We know that greater surface activity leads to decreases in surface tension. When the content of polymer in the system was between 2 wt.% and 8 wt.%, the hydrophobic and hydrophilic regions of molecules were relatively close to each other, showing a relatively loose aggregation state. The surface activity of the system decreased, and the lowest was found at 8 wt.%. The surface tension was highest at 8 wt.%. The hydrophobic regions of the polymer and BSA were completely gathered together, and the surface activity of the system was reduced, so the surface tension increased. When the polymer content of the system increased, the excessive hydrophobic segments in the system were crosslinked, and the surface activity of the system hardly changed. Therefore, as the surface tension of the system decreased from 8 wt.% to 10 wt.%, it became increasingly gentle from 10 wt.% to 14 wt.%.

2.5. Effect of pH Value on the Diameter of P(AA-co-OMA)-BSA Aqueous Solutions

According to Figures 2–4, the combination of P(AA-co-OMA)-BSA aqueous solutions was the best when the P(AA-co-OMA) content was 8 wt.%. The influence of pH value on the P(AA-co-OMA)-BSA aqueous solutions was discussed under the P(AA-co-OMA) content of 8 wt.%. The intensity diameter of the system increased with pH (Figure 5). The COO^- content increased with pH value. When there was more COO^-, it could combine with more BSA, and the particle size of the system increased accordingly.
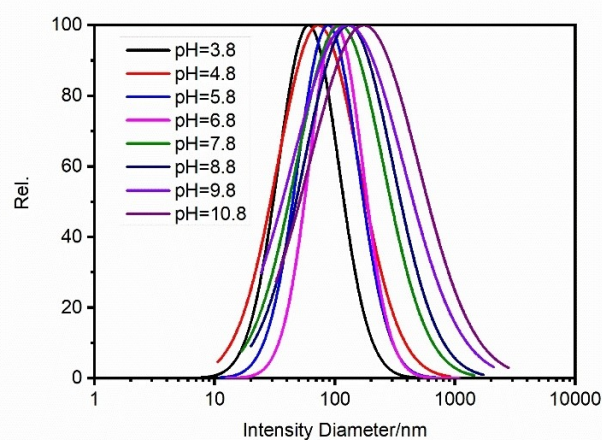

Figure 4. Effect of P(AA-co-OMA) content on surface tension of P(AA-co-OMA)-BSA aqueous solutions.

Figure 5. Effect of pH on the diameter of P(AA-CO-OMA)-BSA aqueous solutions.

2.6. FTIR Characterization of the Molecular Interaction Between Hydrophobically Associating Polymer Poly(acrylic acid-octadecyl methacrylate) and BSA

The 1 wt.% mixed solution with 8% of P(AA-co-OMA) content and pH value of 6.8 was selected and dried at 105 °C for infrared characterization. In this system, the aggregation of polymer and BSA mainly depended on hydrophobic interaction and hydrogen bonding interaction. The carboxylic acid in the polymer and the amino group on the amino acid depended on the hydrogen bonding. The addition of polymer had an impact on the infrared image of BSA, and the groups in the system had a slight displacement.

Figure 6a shows the infrared spectrum of BSA. The absorption peak of amino and carboxyl group on the protein molecule was at 3282 cm^{-1}. The absorption peak at 3325 cm^{-1} shown in Figure 6b was stronger and sharper than that shown in Figure 6a, which was due to the hydrogen bond between the amino group on the BSA protein surface and the carboxyl group in the polymer. In Figure 6b, 2971 cm^{-1} and 2886 cm^{-1} are antisymmetric and symmetric stretching vibrations of the methyl group, and they are stronger than those shown Figure 6a because of the combination of the hydrophobic associating polymer with the protein. The hydrophobic part of the polymer contains long alkane chains. In Figure 6a, 1647 cm^{-1}, 1522 cm^{-1}, and 1241 cm^{-1} represent $-C=O$ stretching vibration, carboxylate bond vibration, and C−N bond vibration, respectively. In Figure 6b, this part of the bond moves slightly to the higher position. Thus, we confirmed the hydrogen bonding interaction of the carboxyl group and the amino group.

2.7. TGA and DSC Characterizations of BSA and its Combination with Hydrophobic Association Polymer Poly (acrylic acid-co-octadecyl methacrylate)

The thermogravimetric curve can be used to analyze the thermal stability of the material. BSA and hydrophobic associa-
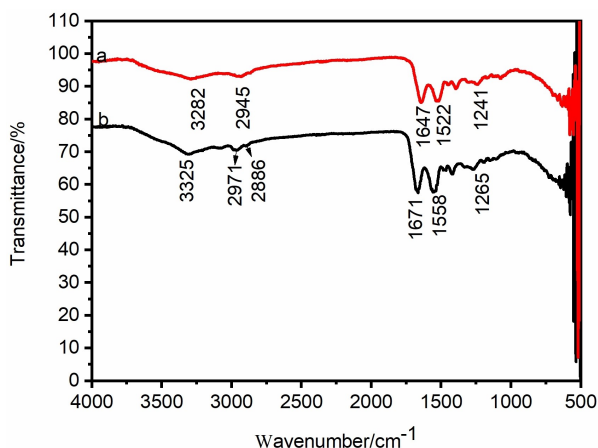
tion polymer poly(acrylic acid-co-octadecyl methacrylate) have hydrogen bonding interaction, and thus the thermal stability of the polymer may change after BSA binding. Figure 7 shows that BSA and P(AA-co-OMA)-BSA lose weight before 126 °C because BSA is a globulin in bovine serum that contains protein, polypeptide, hormone, amino acids, and other components. Therefore, some small molecules in the sample decompose with increasing temperature resulting in weight loss. At the same time, the weight loss of BSA and P(AA-co-OMA)-BSA becomes faster between 207 °C and 210 °C, respectively. The polymer system begins to decompose when it reaches the thermal decomposition temperature. Part of the DTG curve, shown in the figure inset in the TGA curve, shows that the temperature of the fastest weight loss of P(AA-co-OMA)-BSA is 314 °C, which is slightly higher than that of BSA (308 °C). The melting temperature (T_m) was also characterized by the DSC shown in Figure 8. The T_m of P(AA-co-OMA)-BSA moves to 196.3 °C, whereas the T_m of BSA is at 191.6 °C, which indicates that the combination of BSA and P(AA-co-OMA) affects its crystallization. These data suggest that there is a molecular
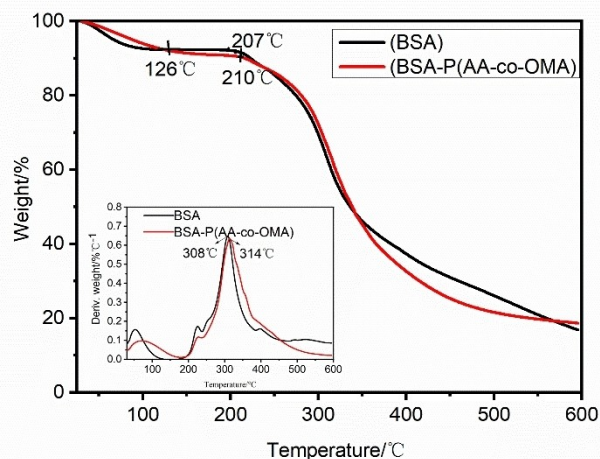
Figure 7. TGA curves and DTG curves (shown in the figure inset) of BSA and P(AA-co-OMA)-BSA.

Figure 6. FTIR spectra of molecular interaction between hydrophobically associating polymer poly(acrylic acid-co-octadecyl methacrylate) and BSA: (a) BSA and (b) binding of BSA to hydrophobically associating polymer poly (acrylic acid-co-octadecyl methacrylate).
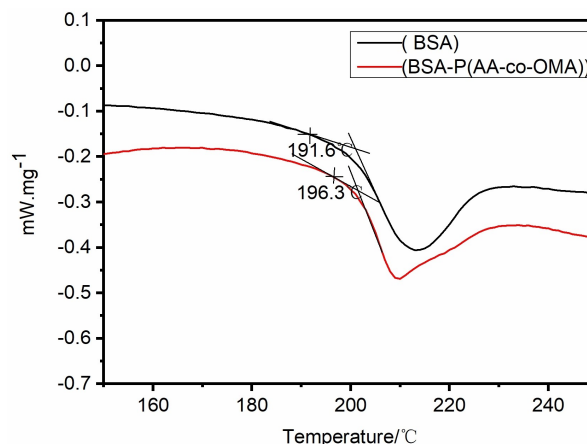
Figure 8. DSC curves of BSA and P(AA-co-OMA)-BSA.

ChemistryOpen

Full Papers
doi.org/10.1002/open.202000336

Chemistry Europe
European Chemical
Societies Publishing

interaction, and the results are consistent with the infrared spectra and TGA curves.

2.8. TEM of 8 wt.% P(AA-co-OMA) in P(AA-co-OMA)/BSA System

We selected the 1 wt.% mixed BSA/P(AA-co-OMA) solution with 8% of P(AA-co-OMA) content and pH value of 6.8. We observed the morphology of the aqueous solution.

Figure 9 shows that the morphology of the aqueous solution of the aggregate is similar to that of the spherical shape, and the aggregation morphology of BSA/P(AA-co-OMA) in the figure is both large and small, which is consistent with the particle size distribution of dynamic light scattering. Because the selected P(AA-co-OMA) is a random copolymer, the distribution of hydrophobic segments in the polymer is not uniform in the molecular structure, which results in the formation of the aggregates after the combination of the system and protein. The TEM figure, however, shows that most of the particle sizes are between 100 nm and 200 nm, and the particle size of the aggregates is affected by the distribution of the polymer's hydrophobic segments. We will study this in the future.
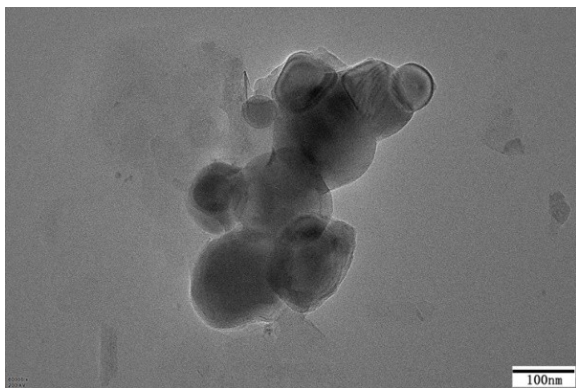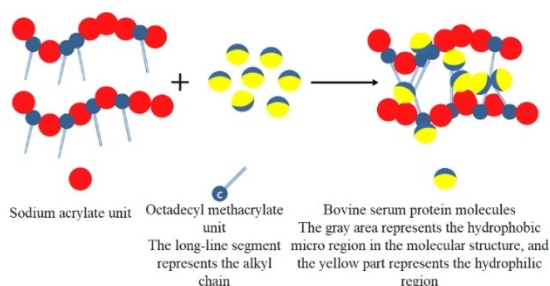

Figure 9. TEM image of P(AA-co-OMA)-BSA.

Sodium acrylate unit   Octadecyl methacrylate unit   Bovine serum protein molecules
The long-line segment represents the alkyl chain   The gray area represents the hydrophobic micro region in the molecular structure, and the yellow part represents the hydrophilic region

Figure 10. Binding mechanism of P(AA-co-OMA) with BSA.

2.9. Analysis of the Binding Mechanism of P(AA-co-OMA) with BSA

P(AA-co-OMA) and BSA molecules mainly combined through hydrophobic and hydrogen bonding interactions. The schematic of the optimum combination of the P(AA-co-OMA) and BSA is shown in Figure 10.

As we know, the hydrophobic chain segment is an irregular block distributed in the P(AA-co-OMA) chain. In this study, the results shown in Figures 2–4 confirm that the aggregation behavior of BSA and P(AA-co-OMA) in aqueous solution depend on hydrophobic interaction. The hydrophobic alkyl chain in the P(AA-co-OMA) extends to the hydrophobic region of BSA to form a hydrophobic inner layer; the hydrophilic chain of P(AA-co-OMA) is in the outer layer to form aggregates. As the P(AA-co-OMA) content continues to increase over 8 wt.%, an excess of hydrophobic chains increases the combination of hydrophobic chains and hydrogen bonds in water. This decreases the surface tension of the P(AA-co-OMA)-BSA aqueous solution. In addition, the carboxylic group in the P(AA-co-OMA) and the amino on the BSA surface are combined by the hydrogen bonding interaction, which is confirmed by the results shown in Figures 6–8.

3. Conclusions

Combining polymers and proteins can be widely useful. Here, we prepared a micro-block graft hydrophobic association water-soluble polymer (P(AA-co-OMA)) and characterized its structure by FTIR. We studied the mechanism between the hydrophobically associating water-soluble polymer and BSA. We also studied zeta potential, dynamic light-scattering particle size, and surface tension of the P(AA-co-OMA)-BSA aqueous solutions. The results showed that the optimal ratio of P(AA-co-OMA) content was found to be 8 wt.%, and the surface tension of 8 wt.% P(AA-co-OMA) content was (70.51 ± 0.46) Mn/m. This analysis showed that the binding between P(AA-co-OMA) and protein depended on the hydrophobic interaction and on the interaction between the hydrophobic chain and protein. We used FTIR to characterize the hydrogen bonding interaction between the polymer and the BSA, and confirmed the results by TGA and DSC. TEM clearly showed the aggregation of BSA and P(AA-co-OMA); we also studied the binding mechanism. Thus, the results offered theoretical support for future improvements in the binding of the polymer with protein, which can be applied in the vaccination field. This research may be useful to immunology in the future. Antigens and P(AA-co-OMA) polymers can also form aggregates and be applied in vaccines.

Experimental Section

Materials

The preparation of poly(acrylic acid-co-octadecyl methacrylate) hydrophobic association aqueous solution was based on the micellar polymerization method, but the emulsifier selected in the system was a composite nonionic surfactant rather than an anionic

ChemistryOpen

Full Papers
doi.org/10.1002/open.202000336

Chemistry Europe
European Chemical
Societies Publishing

surfactant. The synthesis process was as follows: (1) sodium hydroxide neutralized the acrylic monomer; and (2) the hydrophobic monomers octadecyl methacrylate (1% of total monomer mass) and nonionic surfactant were stirred and dissolved in deionized water at 55 °C. Solution (2) was added to (1) under nitrogen. We then increased the rotating speed and stirred for 0.5 h. We increased the temperature of the system to 50 °C–55 °C and started adding ammonium persulfate/sodium bisulfite initiator (0.06% of total monomer mass) dropwise; the temperature rose to about 60 °C. After the initiator was dripped in over 30 min, the system became viscous 0.5–1 h after the general initiator was dripped. The material then was cooled and collected after 6 h of reaction. The viscosity of the polymer aqueous solution (0.5 wt.%) was 12.9 mPa.s,

BSA was purchased from Sigma with a molecular weight (Mw) of 68000. BSA is a spherical protein, and its solubility in water is 100 mg/mL.

Preparation of P(AA-co-OMA)-BSA Aggregate Aqueous Solutions

In this study, we prepared 0.25 wt.% P(AA-co-OMA) aqueous solution and 2.5 wt.% BSA aqueous solution into a 1 wt.% P(AA-co-OMA)-BSA aqueous solution by magnetic stirring at room temperature at 300 r/min with weight fraction ratios of P(AA-co-OMA) in P(AA-co-OMA)/BSA of 2 wt.%, 4 wt.%, 6 wt.%, 8 wt.%, 10 wt.%, 12 wt.%, and 14 wt.%.

We adjusted the pH value of mixtures by hydrochloric acid and sodium hydroxide, respectively. We then studied the binding properties of hydrophobically associating polymer aqueous solution and BSA [P(AA-co-OMA)-BSA] aqueous solution.

Characterization

FTIR characterized the structure of a hydrophobically associating polymer poly(acrylic acid-co-octadecyl methacrylate) produced and its binding behavior with BSA. We used a Perkin-Elmer Spectrum™ (Waltham, MA, USA) 100 FTIR spectrometer and recorded data from 500 to 4000 cm^{-1}.

We measured the thermal decomposition temperature and melting temperature using TGA (Q50, TA Instruments, New Castle, DE, USA) and DSC (DSC214, NETZSCH, Selb, Germany).

We tested the intensity mean diameter and zeta potential of P(AA-co-OMA)-BSA aqueous solutions using a particle sizing system (Z3000, Particle Sizing Systems LLC, Port Richey, FL, USA). In addition, we measured the surface tension of the aggregate aqueous solution using a contact angle measuring instrument (DSA4, KRÜSS GmbH, Hamburg, Germany). We adjusted the pH value of the P(AA-co-OMA)-BSA aqueous solution using an automatic pH acid-base titrator (3 C, INESA Scientific Instrument Co., Ltd., Shanghai, China) and used hydrochloric acid or sodium hydroxide as the acid-base regulator. We characterized the binding morphology of P(AA-co-OMA)-BSA by TEM.

Acknowledgments

Conflict of Interest

The authors declare no conflict of interest.

[1] a) H. Morawetz, H. Sage, *Arch. Biochem. Biophys.* **1955**, *56*, 103–109; b) N. A. Peppas, B. Kim, *J. Drug Deliv. Sci. Tec.* **2006**, *16*, 11–18; c) G. H. Gao, M. J. Park, Y. Li, H. Geun, *Biomaterials* **2012**, *33*, 9157–9164; d) S. Tan, E. M. Campi, R. I. Boysen, K. Saito, *J. Chromatogr. A.* **2020**, *1625*, 461289; e) J. Lv, E. Tan, Y. Wang, Q. Fan, Y. Cheng, *J. Control. Release* **2020**, *320*, 412–420; f) L. Zhang, A. Beatty, L. Lu, A. Abdalrahman, Q. Wang, *Mater. Sci. Eng.* **2020**, *111*, 110768.

[2] a) T. Asimakopoulos, G. Staikos, *Eur. Polym. J.* **2015**, *71*, 567–574; b) L. E. Nita, A. P. Chiriac, M. Bercea, M. Asandulesa, B. A. Wolf, *Int. J. Biol. Macromol.* **2017**, *95*, 412–420.

[3] G. Cavallaro, C. Sardo, E. F. Craparo, B. Porsio, *Int. J. Pharm.* **2017**, *525*, 313–333.

[4] a) S. C. Sarkar, S. C. Shit, D. Q. Dao, J. Lee, *Green Chem.* **2020**, *22*, 2049–2068; b) M. Nihei, T. Nibe, A. M. Putra, *J. Am. Chem. Soc.* **2018**, *140*, 17753–17759; c) S. C. S. R. Paul, T. Fovanna, D. Ferri, B. Srinivasa, *ACS Appl. Mater. Interfaces* **2020**, *12*, 50550–50565.

[5] A. S. Dilgimen, Z. Mustafaeva, M. Demchenko, T. Kaneko, Y. Osada, M. Mustafaev, *Biomaterials* **2001**, *22*, 2383–2392.

[6] D. Xi, *Dissertation, Uni. Lanzhou Jiaotong* **2014**.

[7] a) M. Mustafaev, S. Bayulken, E. Ergen, A. Y. Erkol, N. Ardagil, *Radiat. Phys. Chem.* **2001**, *60*, 567–575; b) M. Mustafaev, S. Sarac, S. Öztürk, *J. Appl. Polym. Sci.* **1996**, *62*, 99–109.

[8] a) L. S. Lakshmi, C. T. Laurencin, *Prog. Polym. Sci.* **2007**, *32*, 762–798; b) T. J. Deming, *Prog. Polym. Sci.* **2007**, *32*, 858–875.

[9] a) N. Nagai, Y. Ito, *Biol. Pharm. B.* **2013**, *37*, 96–104; b) H. D. Xie, M. J. Liu, *Chinese Journal of Animal & Veterinary ences* **2014**, *45*, 2028–2033.

[10] M. Oechsner, S. Keipert, *Eur. J. Pharm. Biopharm.* **1999**, *47*, 113–118.

[11] R. J. Nevagi, M. Skwarczynski, I. Toth, Istvan, *Eur. Poly. J.* **2019**, *114*, 397–410.

[12] a) A. Bettencourt, A. J. Almeida, *J. Microencapsul.* **2012**, *29*, 353–367; b) J. P. Kreuter, P. P. Speiser, *Infect. Immun.* **1976**, *13*, 204–210; c) J. Kreuter, P. P. Speiser, *J. Pharm. Sci.* **1976**, *65*, 1624–1627; d) J. Kreuter, R. Mauler, H. Gruschkau, P. P. Speiser, *Exp. Cell Biol.* **1976**, *44*, 12–19.

[13] a) L. A. Th. Hilgers, l. Nicolas, G. Lejeune, E. Dewil, B. Boon, *Vaccine* **1998**, *16*, 1575–1581; b) L. A. Th. Hilgers, I. Nicolas, G. Lejeune, E. Dewil, B. Boon, *Vet. Immunol. Immunopathol.* **1998**, *66*, 159–171; c) L. A. Th. Hilgers, L. Ghenne, I. Nicolas, M. Fochesato, *Vaccine* **2000**, *18*, 3319–3325; d) W. H. Hussein, P. M. Choi, Z. Cheng, E. Sierecki, *AIMS Allergy Immunol.* **2018**, *2*, 141–147.

[14] a) N. He, R. Wang, *Prog. Chem.* **2012**, *24*, 94–100; b) M. T. Topuzoğulları, N. S. Cimen, Z. Mustafaeva, M. Mustafaev, *Eur. Polym. J.* **2007**, *43*, 2935–2946.

[15] a) M. I. Mustafaev, F. Yucel, S. Ozturk, B. Cirakoglu, E. Bermek, *J. Immunol. Methods* **1996**, *197*, 31–37; b) V. A. Kabanov, *Pure Appl. Chem.* **2004**, *76*, 1659–1677.

[16] F. Petit, R. Audebert, I. Iliopoulos, *Colloid Polym. Sci.* **1995**, *273*, 777–781.

[17] F. Candau, J. Selb, *Adv. Colloid Interface Sci.* **1999**, *79*, 149–172.

[18] a) A. Hashidzume, A. Kawaguchi, A. Tagawa, K. Hyoda, T. Sato, *Macromolecules* **2006**, *39*, 1135–1143; b) G. Baskar, S. Ramya, A. Mandal, *Colloid. Polym. Sci.* **2002**, *280*, 886–891.

[19] S. Bandopadhyay, S. Manchanda, A. Chandra, J. Ali, *P. Drug Delivery Syst.* **2020**, 179–233.

[20] A. Kapse, N. Anup, V. Patel, G. K. Saraogi, D. K. Mishra, *Drug Delivery Syst.* **2020**, 235–289.